Earthquake Time Histories Compatible with the 2005 NBCC Uniform Hazard Spectrum

Gail M. Atkinson

Dept. Earth Sciences, Univ. of Western Ontario, N6A 5B7

gmatkinson@aol.com

Revised Feb. 25, 2009

Can. J. Civil Engineering

Wordcount: 7245

ABSTRACT: The seismic design provisions of the National Building Code of Canada (2005) describe earthquake ground motions for which structures are to be designed in terms of a Uniform Hazard Spectrum (UHS) having a 2% chance of being exceeded in 50 years. The "target" UHS depends on location and site condition, where site condition is described by a classification scheme based on the time-averaged shear-wave velocity in the top 30 m of the deposit. For some applications, such as dynamic analysis by time history methods, it is useful to have time histories that represent the types of earthquake motions expected, and match the target UHS from the NBCC over some prescribed period range. In this study, the stochastic finite-fault method is used to generate earthquake time histories that may be used to match the 2005 NBCC UHS for a range of Canadian sites. Records are provided for site Classes A, C, D and E. They are freely available at www.seismotoolbox.ca .

Keywords: earthquake ground motions, Uniform Hazard Spectrum, NBCC seismic design

INTRODUCTION

The seismic design provisions of the National Building Code of Canada (NBCC 2005) prescribe input earthquake ground motions in terms of a Uniform Hazard Spectrum (UHS) having a 2% chance of being exceeded in 50 years. The UHS provides the response spectrum requirements for structures as a function of vibrational period (where the response spectrum is the maximum response of a single-degree-of-freedom oscillator

with 5% damping). The UHS may be used directly in dynamic analyses to determine seismic response for common methods of linear dynamic analyses, in particular modal analyses. For non-linear analyses, however, time histories of ground motion are required as input. It therefore becomes necessary to obtain earthquake records that are compatible with the NBCC UHS.

There are a number of acceptable methods for obtaining UHS-compatible time histories. For detailed site-specific studies, a common practice is to perform a de-aggregation of the seismic hazard analysis to determine the earthquake magnitudes and distances that contribute most strongly to the hazard (McGuire 1995). Typical contributions include a moderate earthquake occurring nearby, that would be rich in the frequency range that drives short-period oscillators, plus a larger earthquake at greater distance, which would dominate the long-period hazard. Once the scenarios have been identified, appropriate earthquake records are sought for that magnitude and distance, for the site conditions and tectonic region of interest. Spectral matching techniques may be used to improve the match of the natural records to the target spectrum over some desired period range, as described by McGuire et al. (2002) or Hancock et al. (2006), for example. The spectral matching technique has the advantage of allowing real records to be used, and thus ensures realistic information on seismological characteristics such as phasing. There is a concern, however, that the process of spectral matching, which acts to artificially smooth out the natural peaks and troughs of the response spectra of real records, may render them more benign (Luco and Bazzurro 2007). An alternative approach to spectral matching is to generate simulated earthquake records that mimic the seismological characteristics of the expected motions, in terms of frequency content and

duration; the option of using simulated records is particularly attractive if real records with the desired attributes are not available. The use of simulated records also has the advantages of efficiency and flexibility.

Because of the advantages of using simulated records when covering a wide and varied range of scenarios, Atkinson and Beresnev (1998) took this approach in developing UHS-compatible records to match the 1995 NBCC for selected cities. These records have been widely requested and applied. A decade has since past, in which there have been several developments that mandate an update of those simulations. Most significantly, the 2005 NBCC has provided a new target UHS, with a new probability level (2% in 50 years in 2005 as compared to 10% in 50 years in 1995). The target UHS is now specified for a number of standard site conditions, as determined based on shear-wave velocity in the top 30m (V30), or proxy quantities such as blow counts or shear strength. The site conditions range from hard rock (Class A, with V30>1500 m/s) to soft soil (Class E, with V30<180 m/s), with the standard reference condition for the UHS being Class C (V30 360 – 760 m/s). This classification scheme follows that developed for the NEHRP (National Earthquake Hazards Reduction Program) provisions in the United States; its application to NBCC is described by Finn and Wightman (2003). There have also been developments in simulation methods, with stochastic finite-fault methods undergoing significant growth and improvement, including better calibration of the method against actual time-history libraries and seismological observations (Motazedian and Atkinson 2005; Atkinson and Boore 2006; Assatourians and Atkinson 2007; Macias et al. 2008). It is therefore timely to generate new earthquake time histories to match the 2005 NBCC UHS. In this study, I use the stochastic finite-fault

method to generate earthquake time histories that may be scaled (by simple linear scaling) to match the 2005 NBCC UHS for a wide range of Canadian sites. Records are provided for site Classes A, C, D and E. They are freely available from www.seismotoolbox.ca .

METHODOLOGY

Earthquake records that may be used to match the 2005 NBCC UHS at many localities are generated by compiling a comprehensive simulated ground-motion database for earthquakes at the appropriate magnitude and distance ranges, for several generic site conditions. The simulated ground motions are developed from a seismological model of source, path and site parameters that has been validated by comparing data and predictions in data-rich regions. The simulations are based on the well-known stochastic method (Hanks and McGuire 1981; Boore, 1983; Atkinson and Boore 1995, 1997, 2006; Toro et al. 1997; Atkinson and Silva 2000; Boore 2003; Motazedian and Atkinson 2005). The stochastic method begins with the specification of the Fourier spectrum of ground motion as a function of magnitude and distance. Typically the acceleration spectrum is modeled by a spectrum with an ω^2 shape, where ω = angular frequency (Aki 1967; Brune 1970, 1971; Boore 1983, 2003). The "ω^2 model" spectrum is derived for an instantaneous shear dislocation at a point. The acceleration spectrum of the shear wave, $A(f)$, at hypocentral distance R from an earthquake is given by:

[1] $$A(f) = CM_0(2\pi f)^2 / [1 + (f / f_0)^2] \exp(-\pi f \kappa_0) \exp(-\pi f R / Q\beta) / R$$

where M_0 is seismic moment and f_0 is corner frequency, which is given by $f_0 = 4.9 * 10^6 \beta(\Delta\sigma / M_0)^{1/3}$ where $\Delta\sigma$ is stress parameter in bars, M_0 is in dyne-cm, and β is shear-wave velocity in km/s (Boore 1983). The constant $C = \Re_{\theta\phi} FV / (4\pi\rho\beta^3)$, where $\Re_{\theta\phi}$ = radiation pattern (average value of 0.55 for shear waves), F = free-surface amplification (2.0), V = partition onto two horizontal components (0.71), ρ = density, and R = hypocentral distance (Boore 1983). The term $\exp(-\pi f \kappa_0)$ is a high-cut filter to account for near-surface attenuation effects, which describe the commonly observed rapid spectral decay at high frequencies (Anderson and Hough 1984). In the above equation the power of R in the denominator of the attenuation term, $\exp(-\pi fR / Q\beta) / R$, is equal to 1, which is appropriate for body-wave spreading in a whole space. This value can be changed as needed in order to account for deviations from $1/R$ due to factors such as postcritical reflections from the Moho discontinuity or multiply-reflected waves traveling in the crustal waveguide. The quality factor, *Q*(*f*), is an inverse measure of anelastic attenuation . Through this equation, the spectrum is diminished with distance to account for empirically-defined attenuation behavior.

Finite-fault modeling has been an important tool for the prediction of ground motion near the epicenters of large earthquakes (Hartzell 1978; Irikura 1983; Joyner and Boore 1986; Heaton and Hartzell 1986; Somerville et al. 1991; Tumarkin and Archuleta 1994; Zeng et al. 1994; Beresnev and Atkinson 1998). One of the most useful methods to simulate ground motion for a large earthquake is based on the simulation of a number of small earthquakes as subfaults that comprise an extended fault plane. A large fault is divided into N subfaults and each subfault is considered as a small point source (a

method introduced by Hartzell 1978). Ground motions of subfaults, each of which may be calculated by the stochastic point-source method as described above, are summed with a proper time delay in the time domain to obtain the ground motion from the entire fault, $a(t)$:

$$[2] \qquad a(t) = \sum_{i=1}^{nl} \sum_{j=1}^{nw} a_{ij}(t + \Delta t_{ij})$$

where nl and nw are the number of subfaults along the length and width of main fault, respectively ($nl * nw = N$), and Δt_{ij} is the relative time delay for the radiated wave from the ij^{th} subfault to reach the observation point. The $a_{ij}(t)$ are each calculated by the stochastic point-source method (Boore 1983, 2003).

In this study, I use a stochastic finite-fault approach that incorporates significant finite-fault effects such as the geometry of larger ruptures and its effects on ground-motion excitation and attenuation. The simulations are performed with the computer code EXSIM (Extended Finite-Fault Simulation) (Motazedian and Atkinson 2005). This code is an updated version of the FINSIM stochastic finite-fault model code (Beresnev and Atkinson 1997, 2002). The modifications to FINSIM introduce the new concept of a "dynamic corner frequency" that decreases with time as the rupture progresses, to model more closely the effects of finite-fault geometry on the frequency content of radiated ground motions (Motazedian and Atkinson 2005). The model has several significant advantages over previous stochastic finite-fault models, including independence of results from subfault size, conservation of radiated energy, and the ability to have only a portion

of the fault active at any time during the rupture, thus simulating self-healing behavior (eg. Heaton 1990).

EXSIM model parameters that represent the earthquake source processes have been calibrated for crustal earthquakes in active tectonic regions, using data from 27 moderate to large well-recorded earthquakes in California (Motazedian and Atkinson 2005). The calibration process involves deriving the average stress drop parameter, and fine-tuning details of the attenuation model, so that predicted response spectral amplitudes closely match observed response spectral amplitudes, on average, over a wide range of magnitudes and distances. For use in simulating motions from a great mega-thrust earthquake, such as may occur off Canada's west coast, the method has been calibrated using data from the **M**8.3 Tokachi-Oki earthquake in Japan and other large subduction events (Macias et al. 2008). For use in eastern Canada, the model has been calibrated by using information derived from past large events, and from seismographic recordings of small-to-moderate earthquakes (Atkinson and Boore 2006). Calibrated stochastic ground-motion models provide a sound basis for estimating peak ground motions and response spectra for earthquakes of magnitude 4 through 8, at distances from 1 to 500 km over the frequency range 0.2 to 20 Hz. There are other time history generation methods available, ranging from simpler methods to more detailed and comprehensive methods (eg. Somerville et al., 1991). The approach taken here is expedient because the EXSIM program is readily available, has been calibrated for all of the regions of interest in this study, and is suitable for generating a broad range of simulations.

GENERATION OF A REFERENCE TIME HISTORY LIBRARY

The cornerstone of the study is the generation of a comprehensive simulated time history library, including appropriate records for a range of tectonic conditions, earthquake magnitudes, distances and site conditions. The stochastic method outlined above was applied to generate suites of time histories for both eastern and western Canada, for different generic site conditions. Previously developed and validated simulation models, as described below, were used to produce simulated records for a range of magnitudes and distances contributing to hazard at 2% in 50 years. The user may then select records from these suites that may be scaled (using simple linear scaling factors) to match the NBCC target UHS for 2% in 50 years for a specified generic site condition. An electronic catalogue is freely available from www.seismotoolbox.ca that contains all of the simulated time histories, along with their response spectra. The response spectra provide a convenient basis for comparison of the available simulated records with a target UHS, and for derivation of the appropriate scaling factor to match the time history to the target over the selected period range.

Eastern Canada

The simulated records for eastern Canada are generated using the stochastic finite-fault implementation of Atkinson and Boore (2006). Atkinson and Boore (AB06) used the model to develop ground-motion prediction equations for eastern North America (ENA) for rock and B/C boundary conditions. The predictions were validated against records and other seismological data from ENA. The key input assumptions are: (i) the stress drop for ENA earthquakes, which is modeled as a lognormally-distributed random

variable with a mean value of 140 bars; and (ii) the regional attenuation, which follows the empirically-derived regional attenuation model for ENA determined by Atkinson (2004). The fault sizes, as a function of magnitude, are assumed to have the median dimensions as given by the empirical relations of Wells and Coppersmith (1994), but multiplied by a random variable that will result in the average fault area being only 36% of that of a fault of the same magnitude in Western North America (WNA). The reason for the smaller fault sizes in ENA is the high stress drop.

I use the same set of median input parameters as AB06 for the simulations of this study, but modify the treatment of aleatory uncertainty, in two respects. First, all spectral amplitudes are multiplied by an amplification factor of two in the simulation process, in order to provide ground motions for a given magnitude and distance that are about one standard deviation above the median. The reason for the amplification is that typical seismic hazard de-aggregations suggest that most hazard contributions come from motions well above the median (McGuire 1995). Second, aleatory variabilty is reduced and simplified relative to the model used in Atkinson and Boore (2006). Instead of a full consideration of variability in each input parameter, the median values are used, and a random stochastic factor that is uniformly distributed between ±0.1 log units (factor of 1.25) is applied as an amplification (or de-amplification) at 10 selected periods from 0.05 to 10 seconds (the factor is randomly drawn for each selected period, with interpolation being used to determine the factors between the selected points). This preserves the overall median values without too much scatter, but provides some variability in shape from one time history to another. All other simulation parameters are as given in AB06, and the reader is referred to that paper for details.

The key simulation parameters, in particular those that are varied from ENA to WNA, are listed in Table 1. Ground motions for ENA are simulated for moment magnitudes (**M**) 6 at fault distances from 10 to 30 km, and for **M**7 at 15 to 100 km. Hazard de-aggregations (Adams and Atkinson 2003; Halchuk et al. 2007) and preliminary comparison plots indicate that a **M** 6 event in the 10-30 km distance range will match the short-period end of the UHS, while a **M**7 event at a somewhat larger distance (but within the same range) will match the long-period end of the UHS, for cities in eastern Canada in regions of moderate-to-high seismicity. For eastern Canadian sites of low seismicity, records near the large end of the distance range for each magnitude (possibly scaled down) should be appropriate. For each magnitude, I simulate records for two fault-distance ranges: **M**6 at 10 to 15 km (M6 set 1), and 20 to 30 km (M6 set 2); and **M**7 at 15 to 25 km (M7 set 1), and 50 to 100 km (M7 set 2). For each of these record sets, I simulate 3 random components, at 15 randomly drawn locations around the fault, (for a total of 4 sets x 3 components x 15 realizations = 180 simulations for each site condition). The simulations are repeated for hard-rock (A), and for C, D and E conditions. The simulations for site class A (30m shear-wave velocity V30 > 1500 m/s) are based on the AB06 model for hard-rock conditions. To obtain motions on site classes C, D and E, the input model of AB06 for B/C boundary conditions is used, with appropriate soil amplification functions, as described in AB06 (and as taken from Boore and Atkinson 2008) to reproduce motions on C (30m shear-wave velocity V30 = 550 m/s), D (V30 = 250 m/s) and E (V30 = 150 m/s). Note that the amplification functions for D and E sites are nonlinear (Boore and Atkinson 2008), and thus depend on the amplitude level of the input motion. This was accommodated in the simulations by

defining the appropriate non-linear amplification function for the approximate input acceleration level (expected PGA on B/C) for the given magnitude-distance range being simulated; these PGA levels are 0.3 g for the eastern Canadian records of set 1 (M6 at 10-15 km, M7 at 15-25 km) and ≤0.1 g (linear) for set 2 (M6 at 20-30 km and M7 at 50-100 km). The amplification functions are shown on Figure 1. Figure 1 also shows the approximate de-amplification that is implied for site class A, by comparing the simulations on A to those on B/C. Note, however, that the A simulations were derived directly using the appropriate input parameters, rather than obtained by de-amplification of B/C motions.

The suite of simulations described above provides a catalogue of simulated motions for **M**6 and 7 at a range of distances, for sites classes A, C, D and E, from which records to match the UHS may be selected and scaled, as described in the next section.

Figure 2 shows example records, on site class C, for a **M**6 event at 10 to15 km in eastern Canada, in comparison to a **M**6.5 event at the same distance in western Canada. In each case, a 3-component set is shown. Each 3-component record set could be used to represent 3 random horizontal components, or two orthogonal horizontal components plus a vertical component. All records are statistically independent as the random number seed is changed for each trial, but the location of each of the three components in space is the same, as is the fault and hypocenter location. Thus for each of the four scenario sets generated (**M**6 at 10-15 km, **M**6 at 20-30 km, **M**7 at 15-25 km, **M**7 at 50-100 km), the generated records provide 15 3-component sets, or 45 random horizontal components. This allows flexibility in use of the records. It is implicitly assumed that for the level of this analysis, the vertical component can be assumed equal to the

horizontal component on average; alternatively, the user could specify that the vertical target spectrum is given by some fraction of the horizontal factor, such as the value of 2/3 that is often used to specify the vertical from the horizontal. The NBCC does not actually specify or consider a vertical component (except when considering cantilevered systems); it is assumed that vertical loads are not significant in most cases in dynamic analysis as they are not amplified by the structure (Commentary J to NBCC 2005).

Western Canada

For western Canada, the hazard comes from a range of earthquake types. The important contributions to hazard at intermediate-to-high frequencies are moderate-to-large earthquakes in the shallow crust or within the underlying subducting slab (Adams and Halchuk 2003; Adams and Atkinson 2003). At long periods, the potential for great (**M**>8 to 9) megathrust earthquakes on the Cascadia subduction zone is the main concern. Cascadia subduction events are at a significant distance (>100 km) from densely-populated regions, but would produce long-periods motions that would have long duration (>1 minute); the long duration of the motions could be very damaging if structures are pushed beyond their elastic limits. The simulation model for each type of earthquake is described below.

Crustal and In-slab events

The magnitudes used for the simulation of crustal and in-slab events in western Canada are higher than those used for ENA, **M**6.5 and **M**7.5, reflecting the greater contribution to hazard from larger events in B.C. It is assumed that crustal and in-slab events have similar source and attenuation characteristics, based on empirical

observations of ground motions from such events (Atkinson 2005). The simulation parameters for these events are listed in Table 1. They are drawn from consideration of the works of Atkinson (2005) for B.C., and Raoof et al. (1999), Atkinson and Silva (2000) and Motazedian and Atkinson (2005) for California. Motazedian and Atkinson (2005) provided a calibrated stochastic finite-fault simulation model that predicts observed crustal earthquake ground motions in California, while Atkinson (2005) showed that the California model appears to be reasonable for B.C. when differences in site conditions are considered. In this study, I adopt a median stress parameter of 50 bars, with the attenuation model used by Motazedian and Atkinson (2005). As was the case for ENA, I amplify all motions by a factor of two to represent motions near one standard deviation above the median, then apply an aleatory variability factor to the spectral shape, drawn independently at selected periods, from a uniform distribution of ±0.1 log units. Site amplification is treated in the same way as for ENA; the same crustal amplification factors are used in order to simulate motions on A, and for the B/C boundary condition (760 m/s). Likewise, the same amplification functions to go from B/C to C, D or E site conditions are used, in each case using the non-linear amplification factors for the appropriate level of PGA (B/C) from Boore and Atkinson (2008). These reference PGA(B/C) levels are are 0.2 g for set 1 (for **M**6.5 and **M**7.5), and ≤ 0.1 g for set 2. This simplified treatment of site response is appropriate as the motions will be matched to a target UHS that treats site response the same way across the country. Likewise, it could be noted that because the motions will be matched to a target, the stress-drop value of the simulations and the overall amplification factor is also somewhat arbitrary; similar

motions could be obtained using somewhat different stress drops, and then applying different scaling factors to reach the target.

The number of trials and distance range simulated follow the pattern used for ENA. Thus for western Canada, for each site condition, there are 4 sets of 45 records (each of which can be considered as either 45 random horizontal components or 15 3-component sets): **M**6.5 at 10 to 15 km, **M**6.5 at 20 to 30 km, **M**7.5 at 15 to 25 km, and **M**7.5 at 50 to 100 km. Figure 3 shows example records, on NEHRP C, for a **M**6.5 at 13 km and a **M**7.5 at 26 km; an example Cascadia record for **M**9 at 112 km (described in the next section) is shown for comparison. Note that the Cascadia record has relatively low PGA but very long duration, in comparison to local crustal or in-slab events.

Interface events

To simulate motions from a megathrust event on the Cascadia subduction zone, we use the stochastic finite-fault simulation model for Cascadia of Atkinson and Macias (2009). This model was calibrated against the hundreds of strong-motion recordings from the **M**8.3 Tokachi Oki earthquake that occurred in Japan's subduction zone (Macias et al. 2008). The calibration consists of comparing the simulated response spectra to the observed response spectra, and fine-tuning the stress drop parameter, attenuation and site response model to provide a close match between observed and simulated spectra. The calibrated model was modified for Cascadia by using region-specific attenuation (Atkinson 2005; Atkinson and Silva 2000), and a stress drop based on modeling of other worldwide subduction earthquakes, as described by Atkinson and Macias (2009). The simulation parameters are listed in Table 1, but readers are referred to Atkinson and Macias (2009) and Macias et al. (2008) for details of the simulations and validation.

For the time histories for this study, an event of **M**9 was simulated (using the wide "9c" geometry specified by Atkinson and Macias 2009). Simulations were made for distances ranging from 100 to 200 km from the fault. The site conditions and amplification factors are as given in the previous sections (including the overall amplification by a factor of two, and the aleatory variability of ±0.1 log units in shape across selected periods). As the predicted PGA levels are low (<0.1g on B/C site conditions), the site response is essentially linear. Figure 3 includes an example record on site class C at an appropriate distance for use in representing potential motions at Victoria or Vancouver (112 km). Subduction records may not "look" damaging at first glance; they have low PGA values due to their relatively large distances, where distance acts to filter out higher frequencies. However, they have rich energy content at long periods (as will be shown in the next section), and have long durations. These characteristics make them potentially damaging, especially to long-period structures.

MATCHING SIMULATED RECORDS TO A TARGET UHS

The target UHS that we wish to match with the simulated time histories are the UHS for 2% exceedence probability in 50 years as given in the National Building Code of Canada (NBCC 2005). The spectra are given in tables for the reference site condition of C, with prescribed amplification factors to convert to other site conditions. The factors are dependent on the expected response spectra on C, as described by Finn and Wightman (2003). For any target UHS (with associated PGA on C), the user can identify the best records to match it by examining the ratio of the simulated response spectra to the target UHS (both for the appropriate site condition), over the period range of interest

for the appropriate record set; this ratio is referred to as (SA_{targ}/SA_{sim}). The user should compute the mean and standard deviation of (SA_{targ}/SA_{sim}) for each candidate record over the period range of interest. The best records in terms of matching the spectral shape of the target (in the specified period range) will be those with the lowest standard deviation. The mean of (SA_{targ}/SA_{sim}) is the required scaling factor for the record to provide a match on average over the specified period range. To keep the records realistic for the types of events being considered, it is recommended to select simulated records with required scaling factors in the range from 0.5 to 2 (approximately). The lower magnitude in the catalogue (**M**6 for ENA, **M**6.5 for B.C.) should generally be used to match the UHS from periods of 0.5 s to 0.1 s (plus PGA), while the higher magnitude records (**M**7 for ENA, **M**7.5 for B.C.) should be searched to match the UHS from periods of 0.5 to 2 s. The Cascadia **M**9 records provide suitable motions for B.C. for structures with periods of about 1 to 5 seconds, for this type of event. It should be noted that no distinction is made for crustal versus in-slab events in B.C. This is consistent with their use in NBCC (the UHS is a composite of contributions to hazard from both event types). For in-slab events, either the **M**6.5 or **M**7.5 simulations would be suitable for consideration. It is likely that records simulated at a closer distance than the depth of the slab (ie. <50 km) may be needed to match the target UHS, due to its composite nature; alternatively, significant scaling factors may be required, depending on the period range of interest.

A spreadsheet of the response spectra (5% damped PSA) of all simulated records for each record set is provided to facilitate the selection and scaling-factor determination (www.seismotoolbox.ca). The recommended procedure is as follows:

1. Define the target UHS for the appropriate locality and site conditions, based on NBCC 2005 (SA_{targ}).
2. Specify the period range over which you wish to match the target UHS.
3. Select an appropriate record set based on the situation and period range of interest. For example, Set 1 of the east M6 records would be selected for short-period to intermediate-period structures in Montreal, while Set 1 of the west M6.5 records would be selected for a similar structure in Vancouver.
4. For each record within the appropriate set, calculate the ratio (SA_{targ}/SA_{sim}) at every period within the period range of interest (values of SA_{sim} are given in tables at www.seismotoolbox.ca).
5. Calculate the mean and standard deviation of (SA_{targ}/SA_{sim}) over the period range.
6. Select as many records as needed (suggested minimum of five is provided as a guide), picking those with the lowest standard deviation (best shape), but having mean (SA_{targ}/SA_{sim}) in the approximate range from 0.5 to 2 if possible.
7. For each selected record, scale every point of the accelerogram by multiplying by the mean (SA_{targ}/SA_{sim}).

I demonstrate the process in Figure 4, which plots the target UHS for Montreal (site class C) from Adams and Halchuk (2003), along with 5 selected scaled records chosen to match the period range from 0.1 to 1 s; these records were drawn from the east M6 set 1 collection. The engineering modifications to the UHS stipulated in the NBCC (2005) have been implemented for the target UHS. These include capping the response

spectra at a constant value for periods less than 0.2 s, with no specified "return" of the spectrum to the PGA value at low periods. However, for display purposes in the plot, the PGA is shown for reference at a period of 0.02 s, and is connected by an arbitrary line to the UHS spectral cap, plotted to a minimum period of 0.03 s. At long periods, the response spectra is prescribed by NBCC (2005) to fall as 1/period from 2 to 4 s, then have a constant value at greater periods. The average response spectrum of the 5 scaled records is also shown. The selected records provide a reasonable match on average, though they slightly exceed the target spectrum at short periods. Such exceedence will be typical at periods <0.2 s, unless the match is done specifically for short periods. The reason is that the NBCC2005 spectrum is "capped" at periods <0.2 s, while the spectra of earthquakes at near-source distances in eastern Canada continue to rise with decreasing period, to periods as low as about 0.05 s. This can be seen in the shapes of the plotted simulated records. Users may choose to either except this additional spectral content above that required by NBCC, or scale to a lower period range if low periods are of particular importance.

Figure 5 provides a similar demonstration of selected scaled time histories for Vancouver (on C), using the set 1 M6.5 records to match periods of 0.1 to 1 s. For comparison, selected Cascadia M9 records, unscaled, are also shown. Cascadia records were selected that would approximately match the target UHS at periods of 1 to 2 s. Note the rich spectral content of these records at long periods. For periods >1s, these Cascadia records provide much greater response than the selected and scaled **M**6.5 records.

SUMMARY AND CONCLUSION

Simulated earthquake time histories have been generated over a range of magnitudes, distances and site conditions appropriate for matching to target UHS for 2%/50 year probability as given in NBCC 2005 for a range of Canadian localities. The records and their spectra are catalogued in electronic files that are freely available at www.seismotoolbox.ca . To select appropriate records, the user should first define the target UHS for their selected location and site condition, according to NBCC 2005, and identify the period range of interest. Then the user should search the appropriate record set to find records that best match the target, using the step-by-step procedure outlined above. It is recommended to select more than one record for each scenario (5 are used as a guide in the examples provided). Scaling factors should be defined to improve the match of the selected record to the UHS over the specified period range (as shown in Figures 4 and 5). By multiplying the selected time histories from the catalogue by the derived scaling factors, a good match to the UHS can be obtained. If a match is required over a wide period range, then more than one record set should be defined. For example, a moderate event at close distance could be used to match the low-period portion of the spectrum, while a large event at larger distance is used to match the long-period end of the spectrum. Note that in this case both the low-period and high-period scenarios must be applied, though not simultaneously, in order to ensure a match to the UHS over all periods. For cities in coastal B.C., potential motions due to a mega-thrust earthquake along the Cascadia subduction zone should also be considered. Scenario records for a **M**9 megathrust event are given for a range of distances and generic site conditions. While the records provided here may be useful for general studies, detailed site-specific

development of appropriate time histories may be needed for critical or special projects. The records provided here are not intended to take the place of such special studies.

ACKNOWLEDGEMENTS

This work was financially supported by the Natural Sciences and Engineering Research Council of Canada, and by the Canada Foundation for Innovation. The constructive comments of two anonymous reviewers are gratefully acknowledged.

REFERENCES

Adams, J. and Atkinson, G. 2003. Development of seismic hazard maps for the 2003 National Building Code of Canada. Canadian Journal of Civil Engineering, **30:** 255-271.

Adams, J., and Halchuk, S. 2003. Fourth generation seismic hazard maps of Canada: Values for over 650 Canadian localities intended for the 2005 National Building Code of Canada. Geological Survey of Canada Open File 4459 150 pp.

Aki, K. 1967. Scaling law of seismic spectrum, Journal of Geophysical Research, **72:** 1217-1231.

Anderson, J. and Hough, S. 1984. A model for the shape of the Fourier amplitude spectrum of acceleration at high frequencies. Bulletin of the Seismological Society of America, **74**, 1969-1993.

Assatourians, K., and Atkinson, G. 2007. Modeling variable stress drop with the stochastic finite-fault model. Bulletin of the Seismological Society of America, **97:** 1935-1949.

Atkinson, G. 2004. Empirical attenuation of ground motion spectral amplitudes in southeastern Canada and the northeastern United States. Bulletin of the Seismological Society of America, **94:** 1079-1095.

Atkinson, G. 2005. Ground Motions for Earthquakes in southwestern British Columbia and northwestern Washington: Crustal, In-Slab and Offshore Events. Bulletin of the Seismological Society of America, **95:** 1027-1044.

Atkinson, G. and Beresnev, I. 1998. Compatible ground-motion time histories for new national seismic hazard maps. Canadian Journal of Civil Engineering, **25:** 305-318.

Atkinson, G., and Boore, D. 1995. New ground motion relations for eastern North America. Bulletin of the Seismological Society of America **85:** 17-30.

Atkinson, G., and Boore, D. 1997. Stochastic point-source modeling of ground motions in the Cascadia region. Seismological Research Letters, **68:** 74-85.

Atkinson, G. and Boore, D. 2006. Ground motion prediction equations for earthquakes in eastern N orth America. Bulletin of the Seismological Society of America, **96:** 2181-2205.

Atkinson, G. and Macias, M. 2009. Predicted ground motions for great interface earthquakes in the Cascadia subduction zone. Bulletin of the Seismological Society of America, **99:** in press.

Atkinson, G. and Silva, W. 2000. Stochastic modeling of California ground motions. Bulletin of the Seismological Society of America, **90:** 255-274.

Beresnev, I. and Atkinson, G. 1997. Modeling finite fault radiation from the ω^n spectrum. Bulletin of the Seismological Society of America, **87:** 67-84.

Beresnev, I. and Atkinson, G. 1998. Stochastic finite-fault modeling of ground motions from the 1994 Northridge, California earthquake. I. Validation on rock sites. Bulletin of the Seismological Society of America, **88:** 1392-1401.

Beresnev, I. and Atkinson, G. 2002. Source parameters of earthquakes in eastern and western North America based on finite-fault modeling, Bulletin of the Seismological Society of America, **92:** 695-710.

Boore, D. 1983. Stochastic simulation of high-frequency ground motions based on seismological models of the radiated spectra. Bulletin of the Seismological Society of America, **73:** 1865-1894.

Boore, D. 2003. Prediction of ground motion using the stochastic method. Pure and Applied Geophysics, **160:** 635-676.

Boore, D. and Atkinson, G. 2008. Ground-motion prediction equations for the average horizontal component of PGA, PGV, and 5%-damped SA at spectral periods between 0.01s and 10.0 s. Earthquake Spectra, **24:** 99-138.

Brune, J. 1970. Tectonic stress and the spectra of seismic shear waves from earthquakes. Journal of Geophysical Research, **75:** 4997-5009.

Brune, J. 1971. Correction. Journal of Geophysical Research, **76:** 5002.

Finn, L. and Wightman, A. 2003. Ground motion amplification factors for the proposed 2005 edition of the National Building Code of Canada. Canadian Journal of Civil Engineering, **30:** 272-278.

Halchuk, S., Adams, J., and Anglin, F. 2007. Revised deaggregation of seismic hazard for selected Canadian cities. Proceedings of the 9th Canadian Conference on Earthquake Engineering: 420-432.

Hancock, J.,Watson-Lamprey, J., Abrahamson, N., Bommer, J., Markatis, A., McCoy, E., and Mendis, R. 2006. An improved method of matching response spectra of recorded earthquake ground motion using wavelets. Journal of Earthquake Engineering, **10,** Special Issue 1: 67-89.

Hanks, T. and McGuire, R. 1981. The character of high-frequency strong ground motion. Bulletin of the Seismological Society of America, **71:** 2071-2095.

Hartzell, S. 1978. Earthquake aftershocks as Green's functions. Geophysical Research Letters **5:** 1-14.

Heaton, T. 1990. Evidence for and implications of self-healing pulses of slip in earthquake rupture. Physics of the Earth and Planetary Interiors, **64:** 1-20.

Heaton, T., and Hartzell, S. 1986. Source characteristics of hypothetical subduction earthquakes in the Northwestern United States. Bulletin of the Seismological Society of America**, 76:** 675-708.

Irikura, K. 1983. Semi-empirical estimation of strong ground motions during large earthquakes. Bulletin of the Disaster Prevention Research Institute, Kyoto University, **33:** 63-104.

Joyner, W. and Boore, D. 1986. On simulating large earthquakes by Green's function additon of smaller earthquakes. In: Earthquake Source Mechanics. Maurice Ewing Volume 6. Geophysics Monographs, American Geophysical Union, **37**: 269-274.

Luco, N. and Bazzurro, P. 2007. Does amplitude scaling of ground motion records result in biased nonlinear structural drift responses?, Earthquake Engineering and Structural Dynamics, The Journal of the International Association for Earthquake

Engineering and of the International Association for Structural Control, **36:** 1813-1835.

Macias, M., Atkinson, G. and Motazedian, D. 2008. Stochastic finite-fault model of the 2003 **M**8.1 Tokachi-Oki earthquake. Bulletin of the Seismological Society of America, **98:** 1947-1963.

McGuire, R. 1995. Probabilistic seismic hazard analysis and design earthquakes: Closing the loop. Bulletin of the Seismological Society of America, **85:** 1275-1284.

McGuire, R., Silva, W. and Costantino, C. 2002. Technical basis for revision of regulatory guidance on design ground motions: Development of Hazard and risk-consistent seismic spectra for two sites. U.S. Nuclear Regulatory Commission, Report NUREG/CR-6769.

Motazedian, D. and Atkinson, G. 2005. Stochastic finite-fault model based on dynamic corner frequency. Bulletin of the Seismological Society of America, **95:** 995-1010.

National Building Code of Canada 2005. National Research Council, Ottawa.

Raoof, M., Herrmann, R. and Malagnini, L. 1999. Attenuation and excitation of three-component ground motion in sourthern California. Bulletin of the Seismological Society of America, **89:** 888-902.

Siddiqqi, J. and Atkinson, G. 2002. Ground motion amplification at rock sites across Canada, as determined from the horizontal-to-vertical component ratio. Bulletin of the Seismological Society of America **92:** 877-884.

Somerville, P., Sen, M. and Cohee, B. 1991. Simulations of strong ground motions recorded during the 1985 Michoacan, Mexico and Valparaiso, Chile, earthquakes. Bulletin of the Seismological Society of America, **81:** 1-27.

Toro, G., Abrahamson, N. and Schneider, J. 1997. Model of strong ground motion in eastern and central North America: Best estimates and uncertainties. Seismological Research Letters **68:** 41-57.

Toro, G. and McGuire, R. 1987. Calculational procedures for seismic hazard analysis and its uncertainty in the eastern United States. Proceedings of the Third International Conference on Soil Dynamics and Earthquake Engineering, Princeton: 195-206.

Tumarkin, A. and Archuleta, R. 1994. Empirical ground motion prediction. *Annali Di Geofisica,* **37:** 1691-1720.

Wells, D. and Coppersmith, K. 1994. New empirical relationships among magnitude, rupture length, rupture width, rupture area, and surface displacement. Bulletin of the Seismological Society of America **84:** 974-1002.

Zeng, Y., Anderson, J. and Yu, G. 1994. A composite source model for computing realistic synthetic strong ground motions. Geophysical Research Letters, **21:** 725-728.

Table 1 – Summary of Median Parameter values for ground-motion simulations.

Parameter	Median ENA	Median WNA	Cascadia
Stress parameter	140 bars	50 bars	90 bars
Geometric spreading, R^b: b =	-1.3 (1 to 70 km) +0.2 (70 to 130 km) -0.5 (>130 km)	-1.0 (1 to 40 km) -0.5 (>40 km)	-1.0 (1 to 40 km) -0.5 (>40 km)
Distance dependence of duration, d R, d =	0 (1 to 10 km) +0.16 (10 to 70 km) -0.03 (70 to 130 km) +0.04 (>130 km)	+0.10 (all dist)	+0.10 (all dist)
Quality factor	$Q = 893\, f^{0.32}$ ($Q_{minimum}$=1000)	$Q = 180\, f^{0.45}$ ($Q_{minimun}$=150)	$Q = 180\, f^{0.45}$ ($Q_{minimun}$=150)
Fault size	Wells & Coppersmith (1994): 0.6*length, 0.6* width	Wells & Coppersmith (1994)	600 x 150 km

Figure Captions:

Figure 1 – Amplification factors, relative to motions for B/C boundary conditions (760 m/s), for different site conditions. A=hard rock (>1500 m/s). C20 is site class C (360-760 m/s) for 20% PGA (on B/C), D10 is class D (180-360 m/s) for 10% PGA (on B/C), E10 is class E (<180 m/s) for 10% PGA (on B/C). D30 and E30 are amplifications for D at 30%g and E at 30%g.

Figure 2 – Example accelerograms (cm/s^2) for C sites for eastern Canada for M6.0 (set 1) (left) and Western Canada for M6.5 (set 1) (right); a 3-component set is shown. Captions give magnitude and closest distance to fault of each record.

Figure 3 – Example accelerograms (cm/s^2) for Western Canada (Site Class C) for M6.5, 7.5 and 9.0, to show differences in record character and duration with increasing magnitude. Captions give magnitude and closest distance to fault of each record.

Figure 4 – NBCC2005 spectrum for Montreal on NEHRP C (heavy solid line), compared to selected scaled records (with numbers as given in legend) from file east6c1.acc; scale factors are 0.55, 0.74, 0.56, 0.61, and 1.01 for records 1, 13, 15, 18, and 42, respectively. Average PSA for the selected scaled records is also shown. Selected period range for matching is 0.1 – 1 sec.

Figure 5 – NBCC2005 spectrum for Vancouver on NEHRP C (heavy solid line), compared to selected scaled records (with numbers as given in legend) from file west6c1.acc for M6.5 events; scale factors are 0.78, 0.87, 1.19, 0.99, 1.43 for records 1,

2, 26, 31 and 38, respectively. Average PSA for the selected scaled records is also shown. Selected period range for matching for M6.5 is 0.1 – 1 sec. Also shown are PSA for 3 unscaled M9.0 records at distance 112 km (file west9c.acc, #4, 10, 14), selected to have approximate match to NBCC2005 spectrum for periods of 1 to 2 sec.

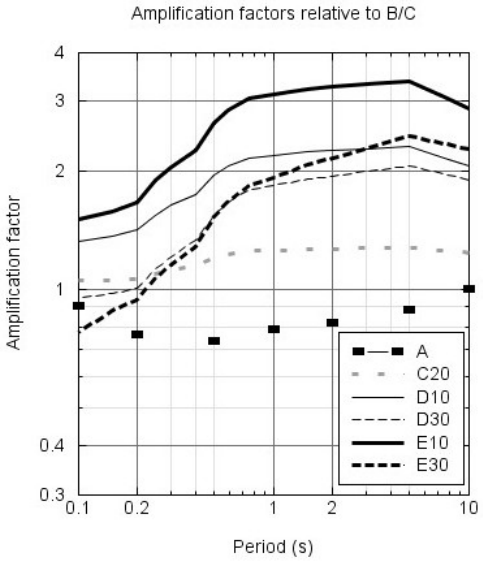

Figure 1 – Amplification factors, relative to motions for B/C boundary conditions (760 m/s), for different site conditions. A=hard rock (>1500 m/s). C20 is site class C (360-760 m/s) for 20% PGA (on B/C), D10 is class D (180-360 m/s) for 10% PGA (on B/C), E10 is class E (<180 m/s) for 10% PGA (on B/C). D30 and E30 are amplifications for D at 30%g and E at 30%g.

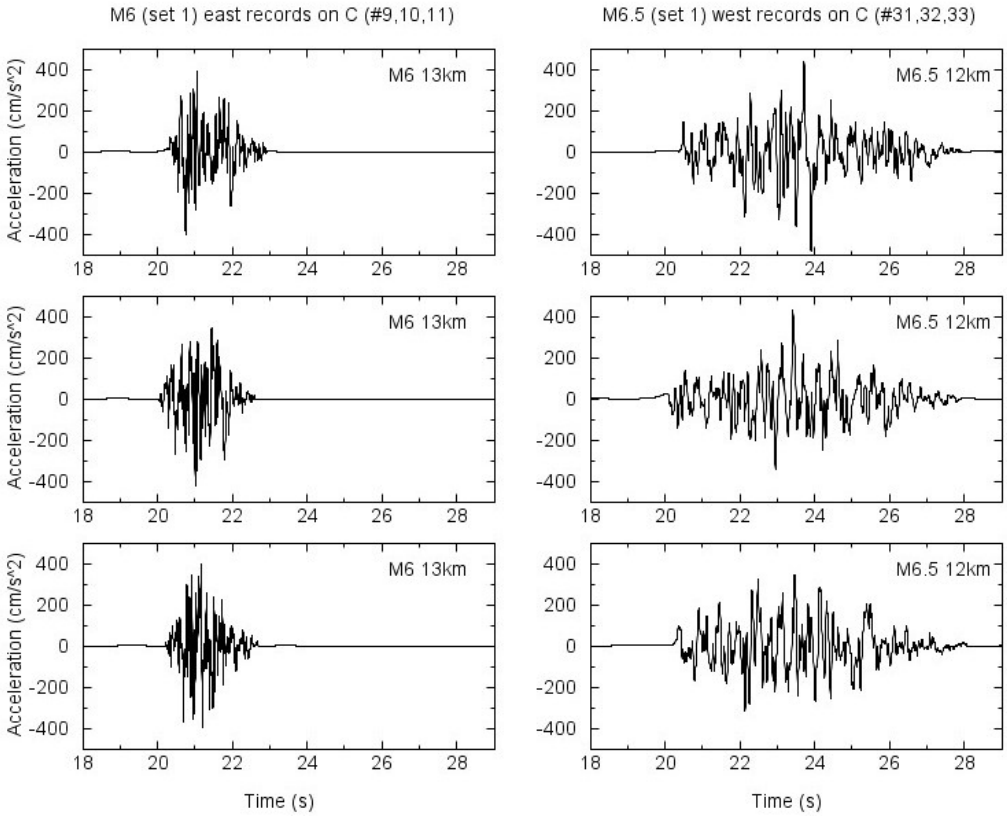

Figure 2 – Example accelerograms (cm/s^2) for C sites for eastern Canada for M6.0 (set 1) (left) and Western Canada for M6.5 (set 1) (right); a 3-component set is shown. Captions give magnitude and closest distance to fault of each record.

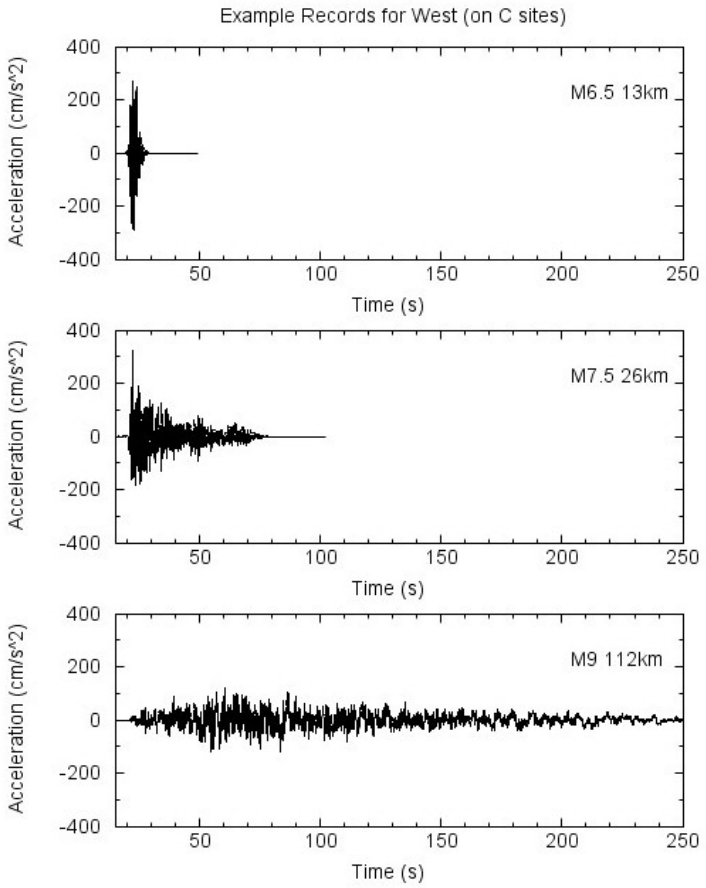

Figure 3 – Example accelerograms (cm/s^2) for Western Canada (Site Class C) for M6.5, 7.5 and 9.0, to show differences in record character and duration with increasing magnitude. Captions give magnitude and closest distance to fault of each record.

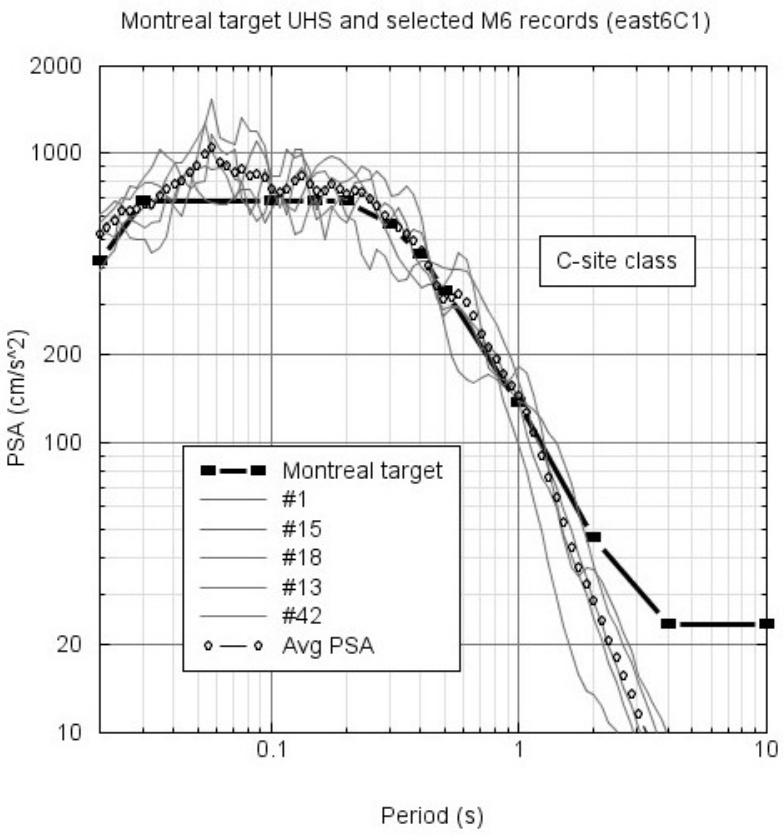

Figure 4 – NBCC2005 spectrum for Montreal on NEHRP C (heavy solid line), compared to selected scaled records (with numbers as given in legend) from file east6c1.acc; scale factors are 0.55, 0.74, 0.56, 0.61, and 1.01 for records 1, 13, 15, 18, and 42, respectively. Average PSA for the selected scaled records is also shown. Selected period range for matching is 0.1 – 1 sec.

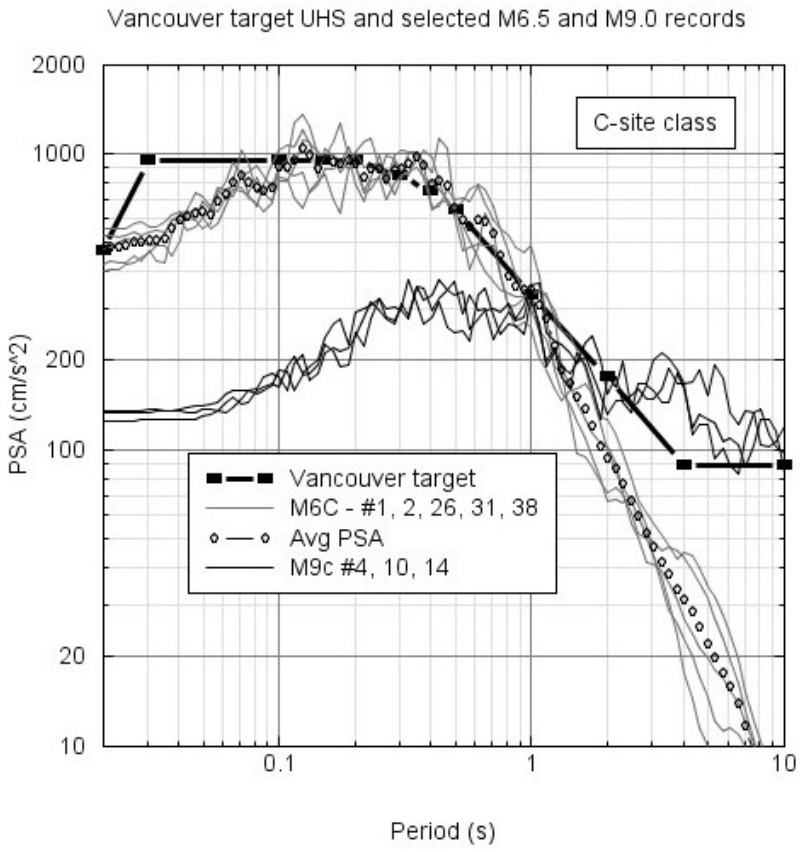

Figure 5 – NBCC2005 spectrum for Vancouver on NEHRP C (heavy solid line), compared to selected scaled records (with numbers as given in legend) from file west6c1.acc for M6.5 events; scale factors are 0.78, 0.87, 1.19, 0.99, 1.43 for records 1, 2, 26, 31 and 38, respectively. Average PSA for the selected scaled records is also shown. Selected period range for matching for M6.5 is 0.1 – 1 sec. Also shown are PSA for 3 unscaled M9.0 records at distance 112 km (file west9c.acc, #4, 10, 14), selected to have approximate match to NBCC2005 spectrum for periods of 1 to 2 sec.